Science in China Ser. D Earth Sciences 2005 Vol.48 Supp. I 172—181

Simulation of CO_2 and latent heat fluxes in the North China Plain

ZHANG Yongqiang[1,2], YU Qiang[1], LIU Changming[1] & WANG Jing[1]

1. Institute of Geographic Sciences and Natural Resources Research, Chinese Academy of Sciences, Beijing 100101, China
2. National Institute for Environmental Studies, Onogawa 16-2, Tsukuba 305-8506, Japan
Correspondence should be addressed to Zhang Yongqiang (email: zhang.yongqiang@nies.go.jp)

Received July 14, 2004; revised January 19, 2005

Abstract We constructed a coupled model for simulating plant photosynthesis and evapotranspiration (CPCEM). In the model, non-rectangular hyperbola is used to simulate leaf photosynthesis rate that is scaled up to estimate canopy gross photosynthesis rate by an integral method. Whole canopy in the model is separated into multi-layers, each of which is divided into sunlit leaves and shade leaves. Canopy net photosynthesis rate is expressed as a function of canopy conductance which is coupled with evapotranspiration. Included the coupled function, evapotranspiration is estimated with a two-layer submodel. The main features of CPCEM are: (1) easy suitability, (2) good physiological base, and (3) simple calculation procedure. Simulated results of CPCEM were compared with those by an eddy covariance system that was installed in a winter wheat farmland of the North China Plain. CPCEM gave a quite well diurnal and seasonal dynamics of net ecosystem exchange, compared with the measurements. The root mean square error between simulation and measurements was only about 2.94 μ mol m^{-2} s^{-1}. Diurnal and seasonal patterns of latent heat flux with the CPCEM were similar to those of measurements. Whereas, simulated latent heat flux was evidently higher than the measured.

Keywords: photosynthesis, canopy conductance, evapotranspiration, coupled model.

DOI: 10.1360/05zd0017

Simulation of plant photosynthesis and evapotranspiration (*ET*) can provide a useful way to evaluate primary production in regional and global scales, to simulate plant growth, to study interaction between land surface processes and climate, and to forecast ecological and environmental changes[1]. There are several kinds of photosynthesis models, including biochemical model, biochemical-energy balance model[2—4], and non-rectangular hyperbola (NRH) model[5—7]. Biochemical model is firstly developed by Farquhar et al.[2]. In the model, photosynthesis rate is limited by rubisco-limited rate of CO_2 assimilation, electron transportation limited CO_2 assimilation rate, and product sink limited rate of CO_2 assimilation. The main feature for the model is evident physiological meaning. Whereas, the model is complicatedly calculated, and iterative calculation should be considered. The response of CO_2 assimilation to environmental factors is usually not included in the model. NRH model considers the response of leaf photosynthesis to irradiance in a NRH way. It needs small parameters to calculate. Only three parameters, light saturated photosynthetic rate, initial quantum efficiency, and curvature factor are included in the model. It gives an excellent phenomenological description of leaf photosynthesis rate[8], and it is easy to be used. As a leaf

model, the NRH model should be scaled up to a canopy model by a reasonable parameterized scheme.

ET can be estimated by a soil-vegetation-atmosphere transfer (SVAT) model. Two-layer SVAT model can separate land surface *ET* into plant transpiration and soil evaporation. Considered physical process of soil and plant and interaction of soil, plant and atmosphere, this kind of model is superior to one-layer SVAT model[9−13].

Considering simplicity and suitability, we use the NRH model to simulate leaf photosynthesis rate, and apply a radiation transfer scheme of canopy to estimating photo synthetically active radiation (PAR) on sunlit and shade leaves, respectively. We separated canopy into several layers to estimate canopy gross photosynthesis rate with an integral method, coupled canopy net photosynthesis rate with canopy conductance with a coupled function, then simulated surface ET with a two-layer submodel. Finally, a coupled plant canopy photosynthesis-canopy conductance-evapotranspiration model (CPCEM) was constructed, which was planed to disclose dynamics of CO_2 and latent heat fluxes. The characters for CPCEM are evident physical meaning, simple calculation procedure, and easy application.

1 The canopy photosynthesis, canopy conductance and evapotranspiration model (CPCEM)

1.1 Energy balance above canopy and on the soil surface

Net radiation (R_n) above canopy can be divided into two parts, R_n absorbed by the canopy (R_{nc}) and R_n absorbed by soil surface (R_{ns}). Energy balance equations above canopy, on the canopy and on the soil surface are

$$R_n = \lambda E + H + G + P_n, \tag{1}$$

$$R_{nc} = \lambda E_c + H_c + S_c, \tag{2}$$

$$R_{ns} = \lambda E_s + H_s - G, \tag{3}$$

where λE is latent heat flux, H is sensible heat flux, G is soil heat flux, P_n is energy flux for plant photosynthesis ignored usually in the energy balance equation, S_c is heat storage in the canopy, which is usually ignored for short height vegetation, e.g. wheat and grasslands, H_c is sensible flux from canopy, H_s is sensible flux from soil surface, λE_c is plant transpiration, and λE_s is soil evaporation. R_n is distributed to R_{nc} and R_{ns} with the Beer-Lambert law. R_n decreases according to an exponent function in the canopy. Thus, the soil surface, R_{ns} becomes

$$R_{ns} = R_n \exp\left(\frac{-\mathrm{EXT}_{rn}\mathrm{LAI}}{(2\cos\delta)^{0.5}}\right), \tag{4}$$

where δ is solar zenith angle, and EXT_{rn} is an extinction coefficient for R_n.

1.2 evapotranspiration submodel

Surface λE is divided into λE_c and λE_s with five kinds of resistances [10]

$$\lambda E = C_c PM_c + C_s PM_s, \tag{5}$$

where PM_c is potential transpiration with entire vegetation cover (no soil evaporation), PM_s is potential soil evaporation with bare soil (no vegetation transpiration), C_c and C_s are resistance coefficients. PM_c and PM_s are estimated from

$$PM_c = \frac{\Delta(R_n - G) + \left[\rho_a C_p VPD - \Delta r_{ac}(R_{ns} - G)\right]/(r_{aa} + r_{ac})}{\Delta + \gamma\left(1 + \frac{r_c}{r_{aa} + r_{ac}}\right)}, \tag{6}$$

$$PM_s = \frac{\Delta(R_n - G) + \left[\rho_a C_p VPD - \Delta r_{as}(R_n - R_{ns})\right]/(r_{aa} + r_{as})}{\Delta + \gamma\left(1 + \frac{r_{ss}}{r_{aa} + r_{as}}\right)}, \tag{7}$$

where Δ is the slope of saturation vapor pressure versus temperature, ρ_a is the air density, C_p is the specific heat at constant pressure, γ is the pyschrometric constant, VPD is vapor pressure deficit at reference height, r_{as} is aerodynamic resistance between the soil and the canopy, r_{aa} is aerodynamic resistance between the

canopy and meteorological level, r_{ss} is soil surface resistance, r_{ac} is canopy boundary layer resistance, and r_c is bulk surface resistance of the canopy (reciprocal of canopy conductance).

C_c and C_s, function of r_{as}, r_{ac}, r_{ss}, r_{aa} and r_c, respectively, can be estimated as

$$C_c = \frac{1}{1+\frac{\xi_c \xi_a}{\xi_s(\xi_c+\xi_a)}}, \tag{8}$$

$$C_s = \frac{1}{1+\frac{\xi_s \xi_a}{\xi_c(\xi_s+\xi_a)}}, \tag{9}$$

where ξ_c, ζ_s, and ζ_a are calculated as

$$\xi_a = (\Delta+\gamma) r_{aa}, \tag{10}$$

$$\xi_s = (\Delta+\gamma) r_{as} + \gamma r_{ss}, \tag{11}$$

$$\xi_c = (\Delta+\gamma) r_{ac} + \gamma r_c. \tag{12}$$

Vapor pressure deficit at the height of sink-source coverage (VPD_0) is determined by total λE

$$VPD_0 = VPD + \frac{r_{aa}}{\rho C_p}\left[\Delta(R_n - G) - (\Delta+\gamma)\lambda E\right], \tag{13}$$

VPD_0 is used to estimate λE_s and λE_c as follows:

$$\lambda E_s = \frac{\Delta(R_{ns}-G) + \rho C_p VPD_0 / r_{as}}{\Delta+\gamma\left(1+\frac{r_{ss}}{r_{as}}\right)}, \tag{14}$$

$$\lambda E_c = \frac{\Delta(R_n - R_{ns}) + \rho C_p VPD_0 / r_{ac}}{\Delta+\gamma\left(1+\frac{r_c}{r_{ac}}\right)}. \tag{15}$$

1.3 A submodel of canopy photosynthesis, canopy resistance and net ecosystem exchange

The NRH is used to estimate leaf photosynthesis rate A_l (μmol CO_2 m^{-2} s^{-1})[7]

$$A_l(\mathrm{PAR}) = \frac{A_m\left[(1+\eta) - \left\{(1+\eta)^2 - 4\varphi\eta\right\}^{0.5}\right]}{(2\varphi)}, \tag{16}$$

where φ is an empirical curvature factor ($0 \leqslant |\varphi| \leqslant 1$), η is an intermediate variable. It is determined by

$$\eta = \frac{\xi\alpha \mathrm{PAR}(L)}{A_m}, \tag{17}$$

where A_m is light saturated photosynthesis rate (μmol CO_2 m^{-2} s^{-1}), L is the depth of leaf area index, PAR(L) is PAR at the depth L, α is initial quantum efficiency (μmol CO_2 /μmol photons), and ξ is the PAR absorption of a leaf.

Canopy is divided into sunlit and shade leaves, on which leaf photosynthesis rate is calculated with NRH, respectively. Then, canopy gross photosynthesis rate is integrated (A_c,molCO_2 m^{-2} s^{-1})

$$A_c = \int_0^{LAI}\left\{f_{slt}(L)A_{l,slt}(L) + f_{shade}(L)A_{l,shade}(L)\right\}dL, \tag{18}$$

where $A_{l,slt}(L)$ and $A_{l,shade}(L)$ are A_l of sunlit and shade leaves in the depth L, respectively, $f_{slt}(L)$ and $f_{shade}(L)$ are the proportion of sunlit and shade leaves, respectively. They are estimated as

$$f_{slt}(L) = \exp\frac{-LG_o}{\mu_0}, \tag{19}$$

$$f_{shade}(L) = 1 - f_{slt}(L), \tag{20}$$

where G_0 is the projection of unit foliage along the direction of incident direct PAR [9], and μ_0 is cosine of solar zenith angle of incident direct PAR.

In soil water stressed environment, soil moisture limits plant photosynthesis, which can be expressed in a nonlinear function[14,15]

$$A_{c,str} = A_c f(\theta), \tag{21}$$

$$f(\theta) = 2\beta(\theta) - \beta^2(\theta), \tag{22}$$

$$\beta(\theta) = \max\left[0, \min\left(1, \frac{\theta-\theta_{wilt}}{\theta_{field}-\theta_{wilt}}\right)\right], \tag{23}$$

where $A_{c,str}$ is A_c in limited soil moisture condition, $f(\theta)$ is an intermediate variable, θ is soil moisture, θ_{wilt} is wilt point, and θ_{field} is field capacity.

Canopy net photosynthesis rate ($A_{n,c}$) is the difference of $A_{c,str}$ to crop autotropic respiration (R_c)

$$A_{n,c} = A_{c,str} - R_c. \quad (24)$$

Net ecosystem exchange (NEE) is the difference of $A_{n,c}$ to soil respiration (R_s)

$$\mathrm{NEE} = A_{n,c} - R_s. \quad (25)$$

In a SVAT model, it is usually difficult to parameterize canopy conductance (reciprocal of r_c). While, it determines CO_2 and H_2O exchange between vegetation and atmosphere. Based on the stomatal conductance model by Leuning et al.[4], a g_c–$A_{n,c}$ function was scaled up to a canopy scale on the study [20]

$$g_c = a' \frac{A_{n,c} P_a}{(C_s - \Gamma^*)\left(1 + \frac{\mathrm{VPD}}{\mathrm{VPD}_0}\right)} + b' \mathrm{LAI}, \quad (26)$$

where a' and b' are coefficients, C_s is CO_2 partial pressure at leaf surface, P_a is atmosphere pressure, Γ^* is CO_2 compensation point, and VPD_0 is empirical coefficient (1500 Pa). C_s is estimated by CO_2 partial pressure of atmosphere (C_a) and leaf boundary conductance (g_b)

$$\frac{C_a - C_s}{P_a} \frac{g_b}{1.4} = A_{n,c}. \quad (27)$$

1.4 Irradiances within the canopy

PAR is divided into direct irradiance and diffuse irradiance. Sunlit leaves receive direct and diffuse irradiance; shade leaves only receive diffuse irradiance. Canopy was divided into 20 layers, each of which was separated into sunlit and shade leaves to calculate irradiance. In the transfer of diffuse radiation, a canopy is idealized to be a plane parallel homogeneous medium. Given a boundary condition on the top of canopy, the equation of diffuse irradiance propagating ($I(L, \mu)$) in the direction μ (cosine of zenith angle) at the depth L is

$$\frac{\mu}{G}\frac{dI}{dL} = -I + \frac{\omega}{2}\int_{-1}^{1} I(\mu')du' + \frac{\omega S_0}{4}\exp\left(\frac{-LG_0}{\mu_0}\right). \quad (28)$$

And the boundary condition is

$$I(0, \mu) = S_d, \quad (29)$$

where G is the projection of unit foliage along the radiance I, ω is the single scattering albedo of a leaf ($\omega = 1 - \xi$), S_0 is the direct PAR on a perpendicular surface at the top of the canopy, and S_d is diffuse PAR irradiance on top of the canopy. The total PAR incident on the canopy is equal to ($S_0\mu_0 + S_d$). A purely absorptive medium would be to consider single scattering within the canopy. In the single scattering approximation, $I(L, \mu)$ satisfying eq. (29) can be changed into the following equation[7,16]:

$$I(L,\mu) = S_d \exp\left(\frac{-LG}{\mu}\right) + \frac{\left(\frac{\omega S_0 G \mu_0}{4}\right)\left[\exp\left(\frac{-LG}{\mu}\right) - \exp\left(\frac{-LG_0}{\mu_0}\right)\right]}{(G_0\mu - G\mu_0)}. \quad (30)$$

The diffuse irradiance on a horizontal surface at the depth L is obtained by integrating $I(L, \mu)$ over the angle as

$$\mathrm{PAR}_{\mathrm{shade}}(L) = 2\int_0^1 I(L,\mu)\mu du, \quad (31)$$

where $\mathrm{PAR}_{\mathrm{shade}}(L)$ is diffuse irradiance at the depth L, where sunlit leaves receive PAR summed up direct and diffuse PAR:

$$\mathrm{PAR}_{\mathrm{slt}}(L) = \mathrm{PAR}_{\mathrm{shade}}(L) + S_0\mu_0. \quad (32)$$

1.5 Plant autotropic respiration

At a certain air temperature (T_a), plant autotropic respiration rate (R_c) is composed of two parts, maintenance respiration rate (R_m) and growth respiration rate (R_g),

$$R_c(T_a) = R_m(T_a) + R_g(T_a), \quad (33)$$

R_m and R_g are controlled by T_a

$$R_m(T_a) = R_{m0} Q_{10}^{(T_a - 20)/10} I_0\left(\frac{1}{2} K \Delta T_a\right), \quad (34)$$

$$R_g(T_a)=(1-Y_G)\{A_{c,str}-R_m(T_a)\}, \quad (35)$$

where R_{m0} is R_m at a reference T_a (20°C), Q_{10} is temperature response coefficient to plant respiration, Y_G is growth conversion efficiency, it is given as 0.74 for wheat[14], I_0 is improved Bessel function, ΔT_a is diurnal variation of T_a, K is logarithm function of Q_{10}.

$$K=\frac{\ln(Q_{10})}{10}. \quad (36)$$

Assumed $1/2K\Delta T=XX$, I_0 is given as a Bessel function:

$$I_0=1+\left(\frac{XX}{2}\right)^2+0.25\left(\frac{XX}{4}\right)^4. \quad (37)$$

Integrating eq. (33) and eq. (35), the total plant respiration is calculated as

$$R_c=(1-Y_G)A_c+Y_G R_m(T_a). \quad (38)$$

1.6 Soil heterotropic respiration

Soil heterotropic respiration (R_s) is exponentially increased with increase of soil surface temperature (T_s)[17]:

$$R_s=R_0 Q'^{\frac{T_s-25}{10}}_{10}, \quad (39)$$

where R_0 is R_s at reference T_s condition (T_s=25℃, R_0=2.5 μmol m^{-2} s^{-1}), Q'_{10} is temperature response coefficient to R_s, which here is given as 1.7.

2 Experiments

Surface λE and CO_2 flux measurements were conducted at Yucheng Comprehensive Experiment Station, Chinese Academy of Sciences (116° 34′13″ E, 36° 50′ N, 28 m a.s.l.), which is located in the North China Plain. Parent materials of the soil are alluvial materials by the Yellow River. Surface soil texture is characterized by light or medium loam soil.

The experiment was carried out in a winter wheat season in 2003. An eddy correlation system was installed at a height of 2.1 m above the soil surface, which basically satisfies the requirement of wind fetch length (installed height/wind fetch length ≈ 1 : 100). The system is composed of a KH-20 hygrometer (Campbell Scientific Inc.), a CSAT3 three-dimension super-anemometer (Campbell Scientific Inc.) and a LI-7500 open CO_2/water vapor infrared analyzer (Li-Cor Scientific Inc.). The hygrometer directly measured λE; the anemometer directly measured H; the LI-7500 infrared analyzer measured λE and CO_2 flux (it is the same as net ecosystem exchange, NEE) at the same time. And, other ancillary data including meteorological, soil moisture data were also simultaneously observed. All data were stored in a Campbell's CR23X data logger at 30-min intervals[18]. Data were collected each week when the system was maintained and checked. Several methods were used to calibrate raw flux data, which include spike removal, coordinate radiation, and WPL correction.

3 CPCEM tests

3.1 Diurnal dynamics and comparison of measured and simulated values

Figure 1 shows the diurnal variation of NEE of measurements and simulation. Negative values mean CO_2 flux downward (sink); positive values mean CO_2 flux upward (source). There was very consistent diurnal variation between simulated NEE and the measured NEE. And peak values of simulation accorded well with the measured NEE.

Diurnal variation of λE by the CPCEM was accorded with that by the measurement (fig. 2). Simulated peak values on the DOY91, DOY95 and DOY96 were higher than those by the measured; simulated peak values were close to measured peak values on the other days. The higher values are probably caused by errors of the CPCEM. Maybe measured peak values are lower than actual λE values because λE values are often underestimated (e.g. energy imbalance) by eddy covariance measurements[19,20]. Lots of studies show that $\lambda E+H$ is only about 60%—90% of available energy (R_n-G)[21,22]. Measurements at 22 ecosystem system stations show that energy imbalance almost existed in all stations, And, average $\lambda E+H$ are 80% of R_n-G[23].Wilson et al.[23] gave five reasons for the energy imbalance including: (1) sample errors associated with different measurement source areas between the

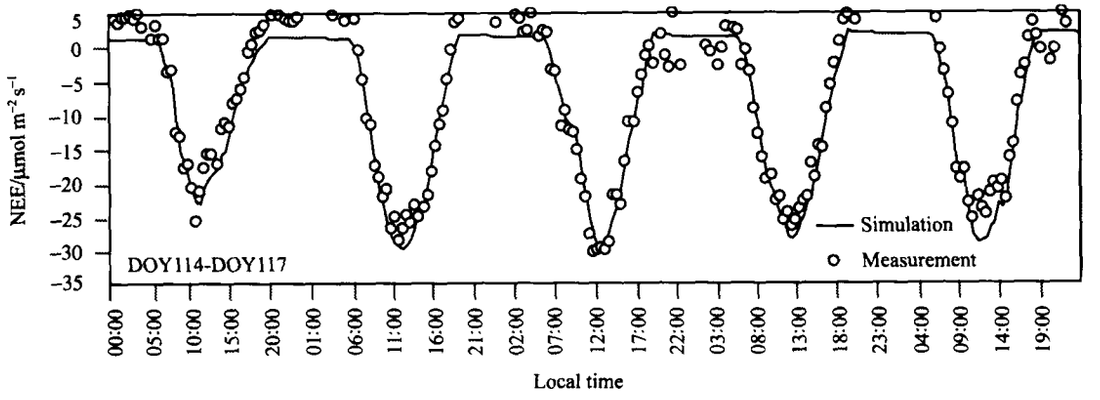

Fig. 1. Diurnal variation of measured and simulated net ecosystem exchanges (NEE) of CO_2. DOY is day of year.

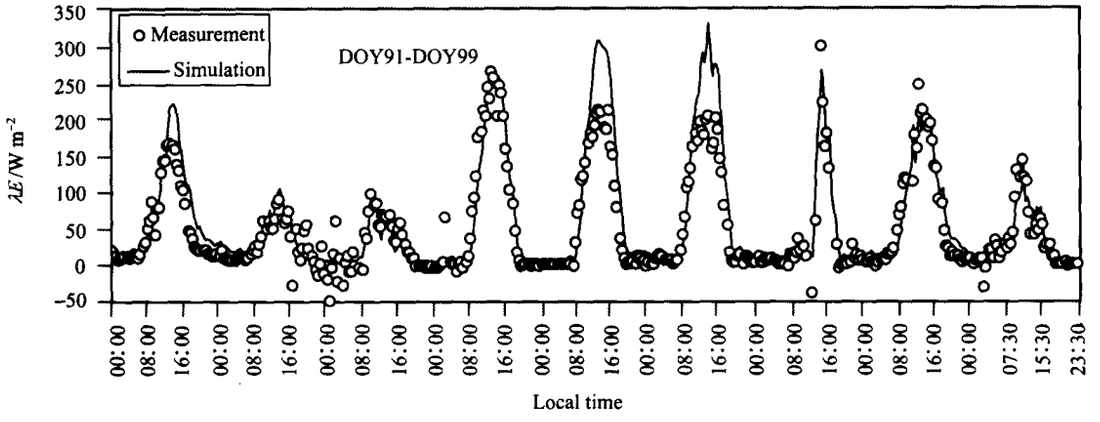

Fig. 2. Diurnal variation of measured and simulated latent heat flux (λE). DOY is day of year.

eddy covariance measurement and the independent available energy measurement, (2) a systematic bias in instrumentation, (3) neglected energy sinks, (4) the loss of low and/or high frequency contributions to the turbulent flux, and (5) neglected advection of scalar[24].

To test the behavior of the CPCEM in different days, we compared measured and simulated NEE in a seasonal scale. Considering strong eddy in daytime, we only chose measured and simulated NEE from 07: 00 to 19:00 (local standard time, LST) to compare with each other. Simulated NEE accorded well quite with measured NEE (slope=1.02, R^2=0.88), with a root mean square error (RMSE) 2.94 μmol m^{-2} s^{-1} (fig. 3). Thus, the CPCEM behaves well in simulating daytime NEE for winter wheat. Similarly, simulated and measured λE were compared from 07:00 to 19: 00 (LST) (fig. 4), simulated λE was correlated well with measured λE (R^2=0.86) with the RMSE about 66.97 Wm^{-2}. Whereas, simulated values are evidently higher than the measured values (slope=1.32). The reasons are the same as the above explanations. During nocturnal periods, friction speed is usually small owing to steady atmospheric condition; eddy material transfer in the vertical direction is very weak. As a result, eddies in the vertical direction are difficult to measure by the eddy covariance system, and ecosystem respiration during nocturnal periods is erroneously measured at the low friction speed[25]. So, we did not compare simulated results with the measurements at that time.

3.2 Seasonal dynamics and comparison of measured and simulated values

By accumulating instantaneous photosynthesis rate and respiration rate, we acquired daily photosynthesis production at sunlit leaves ($A_{c,lit}$) and shade

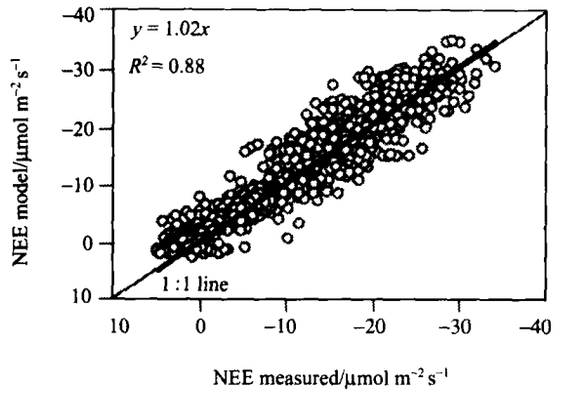

Fig. 3. Comparison of measured NEE values and simulated NEE values. RMSE =2.94 μmol m^{-2} s^{-1} (N=1261), N is number of samples.

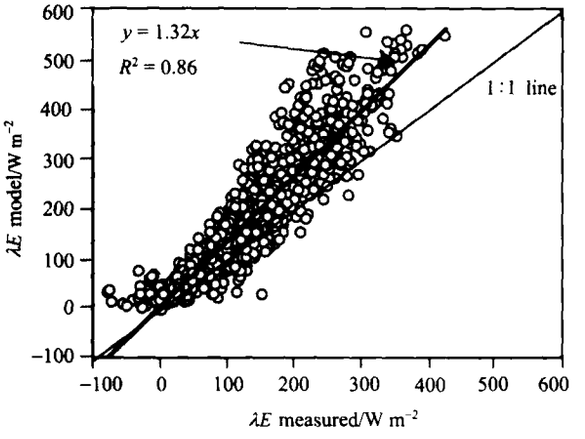

Fig. 4. Comparison of measured latent heat flux (λE) values and simulated λE values. RMSE =266.97 W/m^2 (N=1261), N is number of samples.

leaves ($A_{c,shade}$), daily plant respiration values (R_c). $A_{c,slit}$, $A_{c,\ shade}$, and R_c appeared evident seasonal patterns which are similar to seasonal development of LAI (fig. 5). Highest $A_{c,slit}$ R_c appeared in DOY120-DOY130, when LAI was up to the maximum. Highest R_c appeared slightly after the maximum LAI time. Daily $A_{c,shade}$ was evidently higher than $A_{c,shade}$ whose values are close to those of A_c.

CPCEM simulated $A_{n,c}$ and NEE and measured NEE varied in a similar way to the seasonal variation of LAI. They all increased from the turning-green stage (DOY63) to the heading stage (DOY120), and they were up to peak values during the heading stage to the grain-filling stage (DOY130), and declined after the grain-filling stage (fig. 6)[126]. The maximum $A_{n,c}$ was about 1.0 mol m^{-2} d^{-1}; the maximum NEE was about 0.8 mol m^{-2} d^{-1}. Simulated daily NEE was close to the measured daily NEE, and there was no systematic deviation between them (slope=1.02, R^2=0.83) (fig. 7). The RMSE between them was only 0.089 mol m^{-2} d^{-1}(sample number, N=54).

Simulated daily ET changed seasonally similar to measured daily ET, both of which were accumulated by instantaneous λE values (fig. 8). Daily plant transpiration also appeared the similar seasonal pattern. While daily soil evaporation was mainly decreased at the maximum LAI time. Maximum daily ET with the

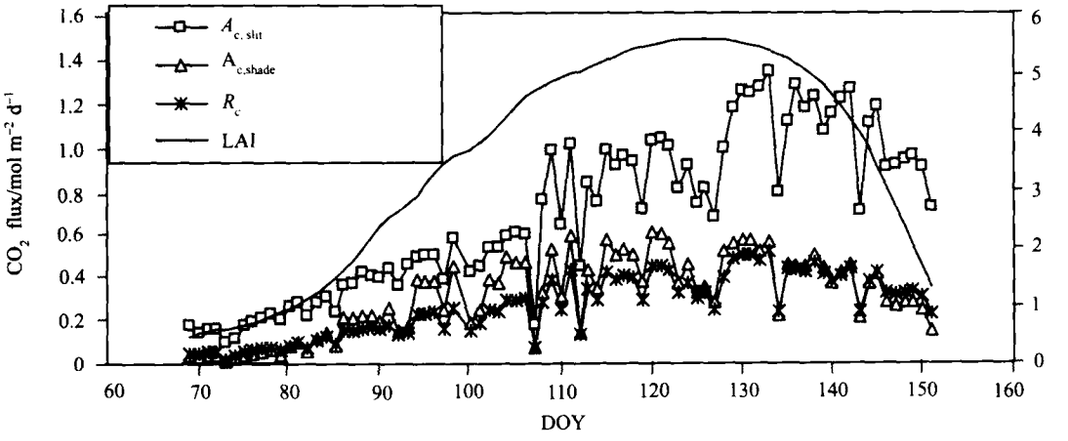

Fig. 5. Seasonal dynamics of photosynthesis rate of sunlit leaves ($A_{c,slit}$), photosynthesis rate of shaded leaves ($A_{c,shade}$), and crop respiration rate (R_c) with the CPCEM.

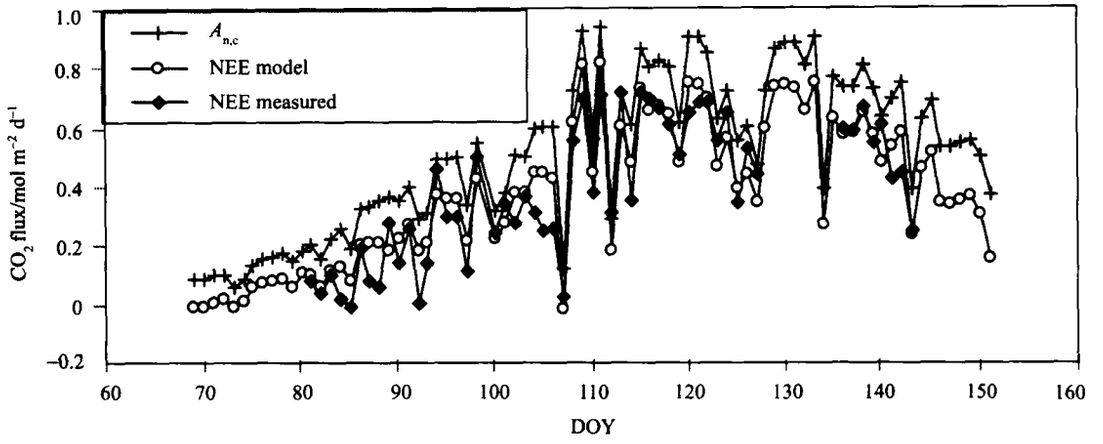

Fig. 6. Seasonal dynamics of canopy net photosynthesis ($A_{n,c}$) and net ecosystem exchange (NEE model) with the CPCEM and measured net ecosystem exchange (NEE measured).

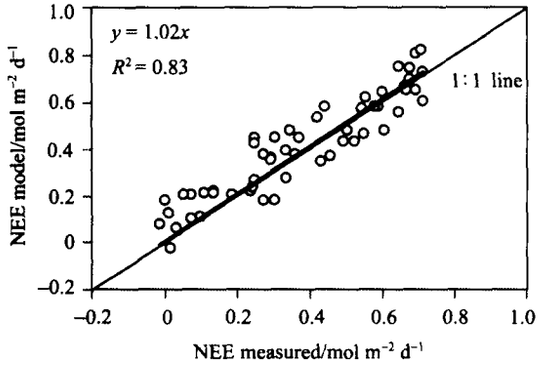

Fig. 7. Comparison of measured (NEE measured) and simulated (NEE model) daily net ecosystem exchange (NEE) RMSE=0.089 mol m^{-2} d^{-1} (N=54), N is number of samples.

CPCEM was about 7.0 mm d^{-1}, which appeared at wheat heading time (about DOY120). Simulated daily *ET* was evidently higher than that of the eddy covariance measurements. While, simulated daily *ET* was highly correlated with measured daily *ET* (R^2=0.81) with RMSE about 1.05 mm d^{-1} (sample number = 54). The reasons of overestimation by the CPCEM can be found above.

4 Result and discussions

In this study, we constructed a coupled plant photosynthesis-canopy conductance-evapotranspiration model (CPCEM) which is used to simulate dynamics

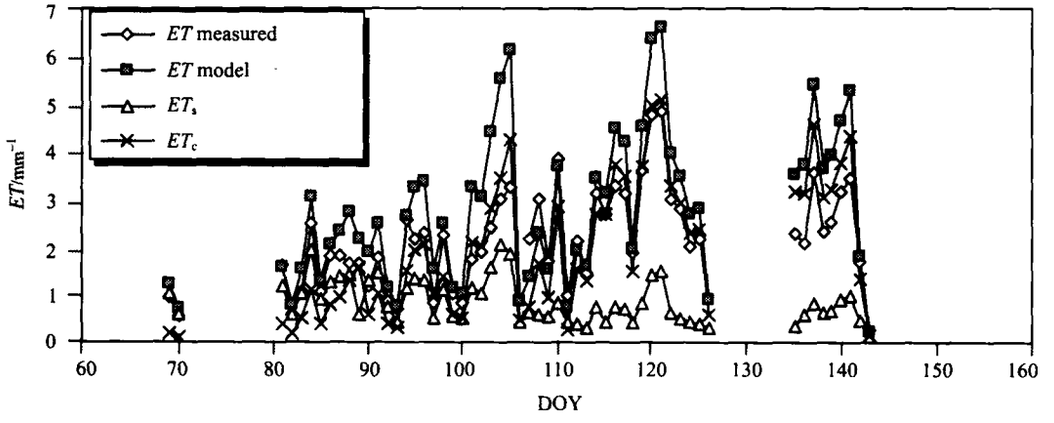

Fig. 8. Seasonal dynamics of daily evapotranpiration (*ET* model), soil evaporation (ET_s), and crop transpiration (ET_c) with the CPCEM and measured daily evapotranpiration (*ET* measured) with the eddy correlation system.

of CO_2 and latent heat fluxes. It was successfully applied to a winter wheat farmland in the North China Plain. NEE by CPCEM was very consistent with the measured NEE. And, CPCEM simulated similar diurnal and seasonal dynamics of ET to those of the measurements, while the simulated ET values were higher than those by the eddy covariance.

Even though CPCEM simulates NEE well, it should be further developed. Here, we only used the semi-empirical Q_{10} way to estimate soil heterotropic respiration (eq. (43)). A mechanism soil respiration submodel should be considered in the CPCEM. λE is usually underestimated by the eddy covariance system, which causes energy imbalance above canopy[27,28]. So, it is difficult to evaluate the accuracy of simulated λE. In further studies, other micrometeorological methods should be simultaneously used to test the CPCEM, which includes Bowen-ratio energy balance method, and aerodynamic method[29,30].

Lots of leaf photosynthesis models are constructed based on the biochemical models. These models are scaled up to canopy and regional scale, and are being used widely[2,31–36]. Biochemical models usually include many parameters, and need iterative methods to solve equations. The NRH was selected in the study, considering its simplicity and suitability. Further, a coupled model was connected with canopy photosynthesis and ET through canopy conductance. Irradiance in the canopy was separated into direct and diffuse irradiances at the sunlit and shade leaves, which was used to the NRH to estimate photosynthesis rate at sunlit and shade leaves, respectively. CPCEM separated canopy into 20 layers to estimate gross photosynthesis rate of each layer, which could greatly improve the estimated accuracy of canopy photosynthesis rate and NEE, compared with one-layer photosynthesis model. The two-layer *ET* submodel was used to simulate plant transpiration, soil evaporation and surface *ET*. This would be a great improvement, compared with the "big leaf" *ET* model.

References

1. Yu, Q,. Xie, X. Q, Sun, S. F. et al., Advancements in simulation of plant photosynthesis production and canopy evapotranspiration, Acta Ecologica Sinica (in Chinese), 1999, 19(5): 744—53.
2. Farquhar, G. D., von Caimmerer, S., Berry, J. A., A biochemical model of photosynthesis CO_2 assimilation in leaves of C_3 species, Plants, 1980, 149: 78—90.
3. Collatz, G. J., Ball. J. T., Grivet, C. et al., Physiological and environmental regulation of stomatal conductance, photosynthesis and transpiration: a model that includes a laminar boundary layer, Agric. For. Meteorol., 1991, 54: 107—136.
4. Leuning, R., Kelliher, F. M., De Pury, D. G. et al., Leaf nitrogen, photosynthesis, conductance and transpiration: scaling from leaves to canopies, Plant Cell Environ., 1995, 18: 1183—1200.
5. Hirose, T., Werger, M. J. A., Maximizing daily canopy photosynthesis with respect to the leaf nitrogen allocation pattern in a canopy, Oecologia, 1987, 72: 520—526.
6. Kull, O., Jarvis, P. G., The role of nitrogen in a simple scheme to scale up photosynthesis from leaf to canopy, Plant, Cell Environ., 1995, 18: 1174—1182.
7. Choudhury, B. J., A sensitivity analysis of the radiation use efficiency for gross photosynthesis and net carbon accumulation by wheat, Agricultural and Forest Meteorology, 2000, 101: 217—234.
8. Thornley, J. H. M., Instantaneous canopy photosynthesis: Analytical expressions for sun and shade leaves based on exponential light decay down the canopy and an acclimated non-rectangular hyperbola for leaf photosynthesis, Annals of Botany, 2002, 89: 451—458.
9. Choudhury, B. J., Monteith, J. L., A four-layer model for the heat budget of homogeneous land surfaces, Q. J. Roy. Meteorol. Soc., 1988, 144: 373—398.
10. Shuttleworth, W. J., Wallace, J. S., Evaporation from sparse crops-an energy combination theory. Q. J. Roy. Meteorol. Soc., 1985, 111: 839—855.
11. Wang, Y., Leuning, R., A two-leaf model for canopy conductance, photosynthesis and partitioning of available energy, I. Model description and comparison with a multi-layered model, Agricultural and Forest Meteorology, 1998, 91: 89—111.
12. Arora, V., Simulating energy and carbon fluxes over winter wheat using coupled land surface and terrestrial ecosystem models, Agricultural and Forest Meteorology, 2003, 118: 21—47.
13. Mo, X. G., Liu, S. X., Simulating evapotranspiration and photosynthesis of winter wheat over the growing season, Agricultural and Forest Meteorology, 2001, 109: 203—222.
14. Amthor, J. S., Respiration and Crop Productivity, New York: Springer, 1989, 339—355.
15. Ronda, R. J., de Bruin, H. A. R., Holtslag, A. A. M., Representation of the canopy conductance in modeling the surface energy budget for low vegetation, J. Appl. Meteorol., 2001, 40(8): 1431—1444.
16. Choudhury, B. J., Estimating gross photosynthesis using satellite and ancillary data: Approach and preliminary results, Remote

Sensing of Environment, 2001, 75: 1—21.
17. Tjoelker, M. G., Oleksyn, J., Reich, P. B., Modelling respiration of vegetation: evidence for a general temperature-dependent Q (10): Global Change Biology, 2001, 7: 223—230.
18. Zhang, Y. Q. Water and heat transfer mechanics in the Soil-Plant-Atmosphere Continuum and regional evapotranspiration Model, Ph. D dissertation of Chinese Academy of Sciences (in Chinese), 2004.
19. Villalobos, F. J., Correction of eddy covariance water vapor flux using additional measurements of temperature, Agric. For. Meteorol., 1997, 88: 77—83.
20. Zhang, Y. Q., Shen, Y. J., Liu, C. M. et al., Measurement and analysis of water, heat and CO_2 flux from a farmland in the North China Plain, Acta Geographica Sinca (in Chinese), 2002, 57(3): 333—342.
21. Constantin, J., Inclan, M. G., Raschendorfer, M., The energy budget of a spruce forest: field measurements and comparison with the forest-land-atmosphere model (FLAME), Journal of Hydrology, 1998, (212—213): 22—35.
22. Kelliher, F. M., Hollinger, D., Schulze, E. D. et al., Evaporation from an eastern Siberian larch forest, Agricultural and Forest Meteorology, 1997, 85: 135—147.
23. Wilson, K., Goldstein, A., Falge, E. et al., Energy balance closure at FLUXNET sites, Agricultural and Forest Meteorology, 2002, 113: 223—243.
24. Kanda, M., Inagaki, A., Letzel, M. O. et al., LES study of the energy imbalance problem with Eddy covariance fluxes, Boundary-Layer Meteorology, 2004, 110, 381—404.
25. Aubinet, M., Grelle, A., Ibrom, A. et al., Estimates of the annual net carbon and water exchange of European forests: the EUROFLUX methodology, Adv. Ecol. Res., 2000, 30: 114—175.
26. Zhang, Y. Q., Eloise, K., Yu, Q. et al., Effect of soil water deficit on evapotranspiration, crop yield, and water use efficiency in the North China Plain, Agricultural Water Management, 64: 107—122.
27. Goulden, M. L., Daube, B. C., Fan, S. M. et al., Physiological responses of a black spruce forest to weather, J. Geophys. Res., 1997, 102(D24): 28987—28996.
28. McCaughey, J. H., Lafleur, P. M., Joiner, D. W. et al., Magnitudes and seasonal patterns of energy, water, and carbon exchanges at a boreal young jack pine forest in the BOREAS northern study area, J. Geophys. Res., 1997, 102(D24): 28997—29007.
29. Zhang, Y., Liu, C., Shen, Y. et al., Measurement of evapotranspiration in a winter wheat field, Hydrological Processes, 2002, 16: 2805—2817.
30. Shen, Y., Kondoh, A., Tang, C., et al., Measurement and analysis of evapotranspiration and surface conductance of a wheat canopy, Hydrological Processes, 2002, 16: 2173—2187.
31. Sellers, P. J., Bounoua, L., Collatz, G. J. et al., Comparison of radiative and physiological effects of doubled atmospheric CO_2 on climate, Science, 1996b, 271: 1402—1406.
32. Sellers, P. J., Randall, D. A., Collatz, G. J. et al., A revised land surface parameterization (SSiB 2) for atmospheric GCMs, Part I. Model formulation, J. Climate, 1996a, 9: 676—705.
33. Pachepsky, L. B., Acock, B., A model 2DLEAF of leaf gas exchange: development, validation, and ecological application, Ecol. Model., 2002, 93: 1—18.
34. Wirtz, K. W., Second order up-scaling: theory and an exercise with a complex photosynthesis model, Ecol. Model, 2000, 126, 59—71.
35. Yu, Q., Liu, J. D., Wang, T. D., Simulation of leaf photosynthesis of winter wheat on Tibetan Plateau and in North China Plain, Ecological Modelling, 2002, 155: 205—216.
36. Zhan, X., Xue, Y., Collatz, G. J., An analytical approach for estimating CO_2 and heat fluxes over the Amazonian region, Ecological Modelling, 2003, 162: 97—117.